Responses of compass neurons in the locust brain to visual motion and leg motor activity

Ronny Rosner[1,2*], Uta Pegel[2,3], Uwe Homberg[2]

[1]Institute of Neuroscience, Newcastle University, Newcastle Upon Tyne, United Kingdom

[2]Department of Biology, Animal Physiology & Center for Mind, Brain and Behavior - CMBB, Philipps-University Marburg, Marburg, Germany

[3]present address: Department of Biology, Case Western Reserve University, Cleveland, OH, USA

***Correspondence:**

Dr. Ronny Rosner
Institute of Neuroscience
Henry Wellcome Building for Neuroecology
Newcastle University
Framlington Place
Newcastle Upon Tyne
NE2 4HH
United Kingdom
ronny.rosner@ncl.ac.uk

Summary statement

In desert locusts, neurons of the central complex, involved in spatial orientation and navigation, change their activity during visual large-field motion and walking activity.

Abstract

The central complex, a group of midline neuropils in the insect brain, plays a key role in spatial orientation and navigation. Work in locusts, crickets, dung beetles, bees, and butterflies suggests that it harbors a network of neurons which determines the orientation of the insect relative to the pattern of polarized light in the blue sky. In locusts, these *compass cells* also respond to simulated approaching objects. Here we investigate in the locust *Schistocerca gregaria* whether compass cells change their activity when the animal experiences large-field visual motion or when the animal is engaged in walking behavior. We recorded intracellularly from these neurons while the tethered animals were allowed to perform walking movements on a slippery surface. We concurrently presented moving grating stimuli from the side or polarized light through a rotating polarizer from above. Large-field motion was combined with the simulation of approaching objects to evaluate whether responses differed from those presented on a stationary background. Here we show for the first time that compass cells are sensitive to large-field motion. Responses to looming stimuli were often more conspicuous during large-field motion. Walking activity influenced spiking rates at all stages of the network. The strength of responses to the plane of polarized light was affected in some compass cells during leg motor activity. The data show that signaling in compass cells of the locust central complex is modulated by visual context and locomotor activity.

Keywords

Central complex, behavioral state, visual motion, insect, compass cells

Introduction

When moving through their environment many animals rely on visual information to orient towards specific targets, to avoid the collision with obstacles, or to make course corrections during long-distance migration. In insects like in vertebrates, specific brain regions are concerned with spatial orientation and navigation tasks. By integrating internal and external sensory information navigation centers in the brain infer the animals' current location and orientation in space and adjust their motor actions accordingly to achieve a desired translocation while also taking into account the animals' current internal and behavioral state.

In insects, the central complex (CX) is a key actor in sensory-motor integration for spatial orientation (Pfeiffer and Homberg, 2014; Turner-Evans and Jayaraman, 2016; Varga et al., 2017; Heinze, 2017). The CX is a group of neuropils that span the brain midline. It consists of the protocerebral bridge (PB), the upper and lower divisions of the central body (CBU, CBL), and the paired noduli (Homberg, 1987; Hanesch et al., 1989; Pfeiffer and Homberg, 2014; Wolff et al., 2014). In many insects, sensory input to the CX is largely visual, and response properties often have a clear navigational context. Strong responsiveness has been found to the angle of polarized light from dorsal directions in field crickets, desert locusts, monarch butterflies, dung beetles, and sweet bees (Vitzthum et al., 2002; Heinze et al., 2009; Sakura et al., 2008; Heinze and Reppert, 2011; el Jundi et al., 2015, Stone et al., 2017), approaching dark objects and small moving targets in locusts (Rosner and Homberg, 2013; Bockhorst and Homberg, 2015b, 2017), wide-field motion in cockroaches, flies and bees (Kathman et al., 2014; Weir et al., 2014, Weir and Dickinson, 2015; Stone et al., 2017) and azimuth-dependent presentation of light spots or vertical bars in flies, beetles,

cockroaches, monarch butterflies, and desert locusts (Heinze and Reppert, 2011; el Jundi et al., 2015; Seelig and Jayaraman, 2013, 2015; Turner-Evans et al., 2017; Varga and Ritzmann, 2016, Weir and Dickinson, 2015; Pegel et al., 2018, 2019). In flies, visual responsiveness of certain CX neurons depends on the animals' behavioral state (Seelig and Jayaraman, 2013, Weir and Dickinson, 2015; Turner-Evans et al., 2017).

The CX harbors numerous cell types (Müller et al., 1997; Heinze and Homberg, 2008; Hanesch et al., 1989; Wolff et al., 2014). However, a picture of which population of neurons codes for which kind of stimuli and to what extent responsiveness depends on a particular behavioral context is just beginning to emerge. One of the best understood networks of neurons within the locust CX encodes heading direction relative to sky compass signals (Pfeiffer and Homberg, 2014; el Jundi et al., 2015; Bockhorst and Homberg, 2015a; Pegel et al., 2018, 2019). The blue sky shows a pattern of polarized light, which is used by many insects for spatial orientation (Horváth and Varjú, 2004; Horváth, 2014). *Compass cells* of the CX are responsive to the angle of polarization, indicated by the orientation of its electric field vector (*E*-vector), and mainly ramify in the PB and the CBL of the CX (Heinze et al., 2009; Homberg et al., 2011; Pegel et al., 2018). In desert locusts, the PB represents *E*-vector orientations in a compass-like manner, presumably determining the orientation of the animal with regard to the sun (Heinze and Homberg, 2007). Compass cells also respond to the simulation of approaching and bypassing objects (Rosner and Homberg, 2013; Bockhorst and Homberg, 2015b), suggesting that they are also involved in collision avoidance. This raises the question of whether additional sensory cues relevant during locomotion as well as internally generated signals during behavior are integrated here to aid in navigation under various behavioral circumstances. We, therefore, tested neurons of the network of compass cells for responsiveness to large-field motion and, in addition, for responses to approaching objects while large-field motion occurred. As the animals were free to move their legs, we

present the first evidence for the involvement of the network in integrating the locust's motor activity state when processing visual information.

Materials and Methods

Animal rearing and preparation

Experiments were performed on 27 adult desert locusts (*Schistocerca gregaria*) of either sex. Animals were reared under crowded conditions at a constant temperature of 28°C and a 12 h light/dark cycle. Animals were mounted vertically on custom-made holders (Fig. 1A), their wings shortened and the hind legs removed. The remaining stumps, the head and mouthparts were immobilized by wax. The fore- and middle legs were free to move. They had tarsal contact with a vertical glass plate below the animal covered with a lubricant (vegetable or silicone oil).

A hole was cut into the anterior head capsule to allow access to the central brain. Tracheal sacs and fat surrounding the brain were removed. The neural sheath was stripped away at the region where the recording electrode was inserted. The gut was removed to prevent pumping movements and, to further stabilize the brain, a wire platform supported the brain from posterior. During recording of neural activity the brain was submerged in locust saline (Clements and May, 1974) containing 0.09 mol l^{-1} saccharose.

Visual stimulation

We provided visual stimuli via two laterally positioned LCD screens (Faytech, Shenzhen, China) and via a rotating polarizer (polarization filter - HN38S, Polaroid, Cambridge, USA; LED light source - ELJ-465-617 - EPIGAP Optoelektronik, Berlin, Germany; rotation speed 30° s^{-1}, visual stimulation angle 3.2°, intensity: 10^{14} photons cm^{-2} s^{-1}) positioned dorsally to the animal (Fig. 1A). Screens had a resolution of 800 x 600 pixels and a frame rate of 75 Hz.

On each side the monitors covered 113° anterior-posteriorly and 127° dorso-ventrally. The Michelson contrast of monitor stimuli was 0.97 calculated with luminances of 70 cd m^{-2} (bright monitor) and 1 cd m^{-2} (dark monitor) measured with an OptiCAL photometer (Cambridge Research Systems, Cambridge, UK). Stimuli were written with MATLAB (MathWorks) using the Psychophysics Toolbox (Brainard, 1997; Pelli, 1997). Light from the displays was depolarized by diffuser sheets mounted in front of the displays. We presented sinusoidal stationary and progressively (backward) moving gratings with a spatial frequency of 1.2 cm/cycle corresponding to 34°/cycle in the screen center. Moving gratings had a temporal frequency of 7.5 cycles s^{-1}. Only for the test of TL2-neuron responses to gratings moving in different directions we used different parameters (horizontal and vertical extent of grating 108°, spatial frequency 53°/cycle, temporal frequency 6 cycles s^{-1}). In several experiments we also presented a dark looming disc stimulus in the center of one of the screens, simulating an approaching object on a collision course. The disc was presented either in front of the stationary or in front of the progressively moving grating background (Fig. 1A). The simulated approaching object had a diameter of 6 cm, started from a virtual distance of 2 meters and approached with a speed of 1 m s^{-1}. The disc stopped expanding 27 ms before the time of theoretical collision when covering a visual angle of 97° and stayed stationary for 500 ms before it disappeared.

Recording procedure

We recorded intracellularly from 27 CX neurons while monitoring leg movements from below with a near infrared sensitive DMK22BUC03 video camera with IC Capture software (The Imaging Source Europe, Bremen, Germany) at 10 fps (Fig. 1A). In some experiments we employed a Dalsa high-speed camera system (Stemmer Imaging, Puchheim, Germany) for evaluation of walking bouts at 100 fps. Each cell was recorded in an individual animal.

24 of those neurons were tested with unpolarized light stimuli. 10 neurons were investigated for responsiveness to polarized light while walking activity occurred. Walking behavior often was not coordinated sufficiently to extract information about directional behavior. We thus restricted our analysis to the presence or absence of leg motor activity during intracellular recordings. In some experiments, we mechanically deflected individual legs with a pin or little brush to test for mechanosensory input to the recorded neurons or elicit walking activity. In order to exclude that visual cues associated with the stimulus were responsible for neural activity changes we moved the brush in the vicinity of the legs without touching them (sham mechanical stimulation).

Microelectrodes were drawn from borosilicate capillaries (1.5 mm outer diameter, Hilgenberg, Malsfeld, Germany) on a microelectrode puller (P-97, Sutter Instrument, Novato, CA). The tips of the electrodes were filled with 4% Neurobiotin (Vector Laboratories) in 1 mol l^{-1} KCl and their shanks with 1 mol l^{-1} KCl. The electrodes had tip resistances of 100–180 MOhm. Signals were amplified (SEC5-LX amplifier; NPI), digitized (CED1401 micro; Cambridge Electronic Design), and stored using a PC with Spike2 software (Cambridge Electronic Design). About 0.25-1 nA of depolarizing current was applied for several minutes to iontophoretically inject Neurobiotin immediately after recording and in some recordings in between the stimulus sequences.

Histology

After completing the physiological recordings, brains were dissected out of the head capsule and fixed overnight in a mixture of 4% paraformaldehyde, 0.25% glutaraldehyde, and 0.2% saturated picric acid in 0.1 mol l^{-1} phosphate buffer. The labeled neurons were made visible for confocal laser scanning microscopy (Leica TCS-SP5; Leica Microsystems) by treatment

of the brains with Cy3-conjugated streptavidin (Dianova, Hamburg, Germany) as described by Rosner and Homberg (2013).

Data analysis

Camera image analysis. Video recordings were analyzed by custom-written software in MATLAB, with Winanalyze tracking software (Mikromak, Berlin, Germany) or Kinovea tracking software (http://www.kinovea.org). In most cases, we determined only brightness changes in the videos without actually tracking individual leg movements, because this procedure proved to be much faster and gave unequivocal information about occurring leg movements. However, for all figures with leg motion data we tracked individual legs, calculated the speed and summed the speeds of the four freely movable legs. We also used the leg speed sum for cross-correlation of the leg motion data (recorded with 100 fps) with spiking data (see below). Before the cross-correlation was calculated we convolved the spike train with a symmetrical triangular window with 10 ms length to estimate the spiking rate. Spiking rate as well as the leg speed trace were normalized by their standard deviations and then fed into the MATLAB xcorr-function. The cross-correlation was normalized by dividing it by the square root of the product of the auto-correlations (xcorr-function option 'coeff'). This has the effect that the auto-correlations at zero lag equal 1.

Anatomical data. Stained neurons were visualized with Amira (version 5.4.5, FEI Visualization Science Group, Mérignac Cedex, France), reconstructed using Adobe Photoshop CC (Adobe Systems, San José, CA, USA), and projected onto a standard CX (el Jundi et al., 2010).

Neuronal responses to unpolarized light stimuli. 24 of the 27 neurons of the study were tested for unpolarized light stimuli. Electrophysiological data were analyzed in MATLAB and Spike2. We employed built-in Spike2 functions for spike detection and visualizing recording traces (DC removal and simple thresholding) and also for visualizing spiking rates. All remaining analysis was done in MATLAB after exporting spike and stimulus times from Spike2.

Statistical significance of responses to grating motion was determined with the Wilcoxon signed rank test (MATLAB signrank function). We averaged spike trains without leg motion across all trials for each cell. One of the 24 animals that were tested with moving gratings showed leg movements in all trials and was thus excluded from data evaluation. The differences in spike number before grating motion onset and during grating motion were compared in the following way: We calculated the number of spikes within three 1 s time windows. Time window 1 started 3 s before grating motion onset, window 2 started 1 s before motion onset and time window 3 started 1 s after motion onset. Thus, time windows 1 and 3 were symmetrical to time window 2. We calculated the difference of spike numbers between time windows 2 and 1 and, additionally, between 2 and 3. Then the absolute values for both differences were calculated for each cell and the resulting values were used in the statistical test. Because this analysis only determines whether the average compass cell responds to grating motion without determining whether a particular cell was inhibited or excited, we employed another procedure to determine inhibitory and excitatory responses. For this we Gauss filtered (SD 200 ms, window size 1 s) average spike trains for each cell and determined the average spiking rate (± SD) within a 2 s time window starting 2.5 s before grating motion onset. A cell was determined to be inhibited (or excited) if its average spiking rate was 3 (background-) SDs below (or above) its average background response continuously for at least 750 ms after grating motion onset. This allowed assessing the

responses of neurons with different response latencies and dynamics. We refer to cells that were neither inhibited nor excited as non-responsive.

For determining average responses across cells we accounted for different background spiking rates in different neurons by subtracting the average background activities from the Gauss filtered traces. Because inhibitory and excitatory responses occurred in different recordings even from the same cell type, we inverted inhibitory responses by calculating the absolute value of the Gauss filtered traces. Finally, the average across cells was calculated.

Looming responses for individual cells were determined similar to moving grating responses: Gauss filtered average spike trains for each cell were calculated and the average spiking rate (± SD) within a 2 s time window starting 2.5 s before looming onset was determined. A cell was determined to be inhibited (or excited) by a looming stimulus if a nadir (or peak) response, that deviated by more than 4 (background-) SDs from the average, occurred within a time window from 1.5 s – 2.5 s after looming onset. This time window corresponds to the typical occurrence of looming responses found by Rosner and Homberg (2013).

Responses to polarized light. We evaluated the responsiveness of neurons to the plane of polarized light using a circular linear correlation analysis (Berens, 2009; Bockhorst and Homberg, 2015a). In a first step we pooled trials with identical stimulus configuration (same direction of polarization filter rotation during walking and without walking). We calculated stimulus-response curves by dividing the pooled spike trains recorded during a full rotation of the polarization filter into 36 bins (10° bin width). In each bin the average spiking activity was calculated. The angular-linear correlation was determined by using the angles of the polarization filter/*E*-vector in the center of each bin as the angular variable and the average spiking activities within the bins as the linear variable (Zar, 1999; Berens, 2009). The

criterion for responsiveness was the significance of the resulting correlation coefficient (α = 0.05). The corresponding p-value was determined as described in detail in Berens (2009).

Neurons that are sensitive to polarized light typically show a sinusoidal oscillation of firing rate with a period of 180° of the rotation of the polarizer. Thus, to determine the strength of the response to the rotating *E*-vector we calculated the amplitude of this frequency component by determining amplitude spectra of firing rates after the curves had been smoothed with our Gauss filter (SD 200 ms) and the average spiking rate had been subtracted. When comparing amplitudes of trials during walking activity of the animals with those without walking activity, we evaluated all trials with walking activity against the same number of trials without walking activity. For comparison, we selected trials without walking activity that were closest to those with walking activity.

Results

We studied the responses of 27 neurons with arborizations in the central complex (CX) of the locust brain. All neurons are part of a network of compass neurons that are sensitive to the oscillation plane of polarized light (Heinze and Homberg, 2009; Heinze et al., 2009). The responses of these neurons to large-field visual motion with and without concurrent presentation of a looming disc and/or to polarized light with and without concurrently occurring leg motion were analyzed. We studied cells at each level of information processing (Fig. 1B; Table 1) including inputs into the CX mediated by tangential neurons of the CBL (TL2 neurons), intermediate neurons, i.e. columnar neurons connecting the CBL to the PB (CL1 neurons) and tangential neurons of the PB (TB1 neurons), and output cells projecting from the PB to the lateral accessory lobes (CPU neurons).

Responsiveness to visual motion

Bilateral presentation of moving gratings resulted in activity changes in neurons at all levels of the polarization-vison network in the locust CX (Table 1). In two recordings from TL2 neurons, a range of translatory and rotatory moving grating stimuli were presented to both eyes (Fig. 2). Irrespective of movement direction, one of the two neurons showed inhibitory responses (Fig. 2C), while the second TL2 neuron was excited (Fig. 2D). In these and other experiments, some (Fig. 2C) or all stimulus presentations (Fig. 2D) were accompanied by leg movements elicited by the moving gratings.

Except for the two TL2 neurons, all other neurons were almost exclusively studied for effects of translational front to back (progressive) motion as experienced by a forward-moving animal. Only in a few cases we also shortly tested regressive large-field motion which gave qualitatively the same results as progressive motion stimulation (not shown). This means neurons that were excited (inhibited) by progressive motion were also excited (inhibited) by regressive motion. To differentiate between visually elicited and motor activity related neuronal responses we excluded trials with leg movements from the analysis. As illustrated in Fig. 2, responses to the moving grating could differ substantially between different representatives of the same cell type (see also Table 1) but were consistent across trials in a given recording. In TL2 neurons, CL1 neurons and TB1 neurons we found representatives that were excited or inhibited, while of the three CPU neurons tested two were not responsive to the stimulus and the third one was excited. In order to evaluate the responses across different recordings statistically, we therefore had to normalize the recordings to identical activity levels before start of grating motion and, further, to invert inhibitory responses for pooling with excitatory responses (see Materials and Methods). Following these procedures, the average responses had a similar phasic-tonic dynamic profile

in all cell types with strong response onset and a gradual decay of response amplitude over the following 4 s (Fig. 3). Statistical evaluation of spiking activities in symmetrical time windows before and after motion onset revealed significance of responses across the recordings (Fig. 3; Wilcoxon signed rank test, n = 23, p = 0.0008).

To investigate whether large-field motion has an effect on the response to an approaching object, we combined stimulation by bilaterally moving gratings with looming stimulation on one side of the animal. Average responses to the monocular looming stimulation occurred later in time when the looming disc was presented in front of a moving grating instead of a stationary one (Fig. 4). In some recordings the responses to the looming stimulus were opposite to those to the moving grating (Fig. 5, Table 1). This means that grating motion was inhibitory while looming was excitatory (Fig. 5A-E) or vice versa (Fig. 5F). In some cases looming responses became only obvious during concurrent large-field motion (Fig. 5C).

Influence of leg motor activity on neuronal activity

An influence of motor activity on neuronal activity of compass neurons could be observed at all levels from input (Fig. 2; TL2 neurons) over intermediate stages (Fig. 6; CL1 neuron) to output (Fig. 7A; CPU1 neuron) even though not every neuron was affected by motor activity. Leg motor activity had an inhibitory effect on background activity in a TL2 neuron and during visual motion stimulation (Fig. 2C). The neuron was also inhibited by grating motion, and inhibition was strongest, when grating motion and leg motion occurred concurrently. The CL1 neuron in Fig. 6 was excited when leg movements occurred spontaneously or were elicited mechanically. The excitations occurred on a short time scale, roughly corresponding to the duration of individual leg movements (Fig. 6B). The average

cross-correlogram (Fig. 6C), from three high speed recordings of leg movements and the corresponding spike rate, peaks 30 ms after leg motion.

We tested 8 labeled neurons for their responses to visual stimulation through a rotating polarizer during walking-like behavior and included two further neurons in our analysis whose morphological identity is not known owing to unsuccessful staining. The results were diverse and no clear picture across all cells emerged. However, in some cells motor activity of the animal was clearly correlated with an increase in response amplitude to polarized light (Fig. 7). A CPU1 neuron responded more strongly when the animal was walking, and the response was weaker again after walking had stopped (Fig. 7A). Similarly for the two neurons of unknown type the responses became stronger during walking, were reduced in amplitude when the animals stopped walking and increased again when the locust went on walking (Fig. 7D,F). One of the four remaining responsive cells, a CL1 neuron, responded only significantly to the polarizer rotation when the animal was motionless but not when it was walking, and while the other three cells responded more strongly during walking, overlapping SEMs of the amplitude spectra indicate that the differences were not statistically significant.

Discussion

We show here that locust compass cells comprising the neural network for processing polarized light information are also responsive to large-field motion. Responses to looming stimuli in front of moving gratings were often opposite to responses to the large-field motion alone making looming stimulus responses more salient. Walking activity often influenced spiking rates at all stages of the network, and some neurons responded more strongly to polarized light stimulation during ongoing leg motor activity.

Relation to other studies

Sensitivity of CX neurons to large-field motion has been reported in three other species, the cockroach *Blaberus* (Kathman et al., 2014), the fruitfly *Drosophila* (Weir et al., 2014; Weir and Dickinson, 2015), and the sweat bee *Megalopta* (Stone et al., 2017). However, in the cockroach and fly the types of neurons were not determined or were of different type from those presented here. In our study all cells investigated belong to what Stone et al. (2017) referred to as compass cells, because of their proposed function in determining heading direction relative to the outside world. Stone et al. (2017) did not find distinctive responses to large-field motion in compass neurons in the bee. Instead they discovered a new class of neurons, characterized by directionally selective sensitivity to translatory large-field motion. Those neurons ramified in the noduli, a subcompartment of the CX. In contrast to the results in the bee many compass cells in the locust responded vigorously to moving gratings. This discrepancy might be due to species-specific differences but could also be based on differences in stimulation such as different temporal frequencies tested.

Relevance and origin of large-field and looming sensitivity

The types of neuron studied here are sensitive to the angle of zenithal polarized light (Heinze et al., 2009). They probably play a role in navigation during migratory flights under the open sky where scattering of sunlight gives rise to a pattern of polarized light. It is conceivable that the neurons are also involved in course stabilization by exploiting optic flow information. Alternatively, optic flow might be an indicator for ongoing motion without being evaluated for any directional information content. In this study we presented large-field motion concurrently to both eyes but did not test monocular stimulation. If cells responded differently to large-field motion to the left and right eye, it might explain why neurons of the

same type showed inhibitory and excitatory responses. Stimulating the left and right eye concurrently could yield an inhibitory or excitatory response, depending on which eye is the dominant one. Different contributions of both eyes to the overall response could be useful in balancing the optic flow experienced by the locust. This balancing of optic flow on both sides is well known from bees (Srinivasan et al., 1991).

Large-field motion-sensitive neurons in the locust optic lobe have been characterized by Rind (1990), Gewecke and Hou (1993) and Homberg and Würden (1997). The neurons studied by Rind (1990) and Gewecke and Hou (1993) ramified within the lobula complex. They were directionally selective and thus behaved like lobula plate tangential cells in flies (Hausen, 1981; Hengstenberg, 1982). Our recordings from TL neurons (Fig. 2) suggest that CX neurons of the polarization-vision network are not directionally sensitive. Therefore, the non-directionally sensitive neurons recorded by Homberg and Würden (1997) are more likely candidates for providing input to the neuronal network investigated here.

Several compass cells responded to looming and moving grating stimulation with opposite sign or became sensitive to looming stimuli only during moving grating stimulation. This behavior of the neurons could play a role during flight in a large swarm when the animals experience large-field motion and at the same time need to avoid collision with conspecifics or obstacles. The origin of the opposite sign of looming and moving grating response is not clear but could be due to separate neuronal pathways feeding into the CX network or rebound effects due to the disc blocking out grating motion in part of the visual field and looming stop during the stationary disc phase. This would also explain why the average absolute responses to looming stimulation in front of a moving grating occurred later than responses to looming stimulation in front of a stationary grating.

Locomotor state dependence of visual responses

Some neurons showed a remarkable increase in responsiveness to the angle of polarized light while walking-like behavior occurred, similar to an increased responsiveness to unpolarized light stimuli during flight within the fan-shaped body of flies (Weir and Dickinson, 2015). Responses of visual interneurons in the optic lobes of locusts and flies had earlier been found to depend on the animals' arousal or motor activity state (Rind et al., 2008; Chiappe et al., 2010; Maimon et al., 2010; Rosner et al., 2010). In locusts an identified looming-sensitive neuron is less prone to habituation in an elevated arousal state (Rind et al., 2008) and thus presumably keeps the animal responsive to imminent collisions during locomotion. In flies a rather complex picture of state dependent visual responses has emerged. The amplitude of head optomotor responses to large-field motion is largely increased during locomotor activity, and the responsible gain modulation was concluded to be mediated downstream of the visual system (Rosner et al., 2009; Haag et al., 2010; Rosner and Warzecha, 2011). However, even at an earlier stage, at the level of visual interneurons mediating these optomotor responses, state dependent modulation takes place (Chiappe et al., 2010; Maimon et al., 2010; Rosner et al., 2010; Jung et al., 2011; Rien et al., 2012). The effect of locomotor activity on visual interneurons is mediated by octopamine in flies (Longden and Krapp, 2009; Suver et al., 2012) and locusts (Bacon et al., 1995; Stern, 1999; Rind et al., 2008) as had been found earlier for bees (Kloppenburg and Erber, 1995). The response changes within and downstream of the visual system are mediated by a central signal rather than by proprioceptive feedback (Rosner et al., 2009; Haag et al., 2010; Rosner et al., 2010; Fujiwara et al., 2017). Similar to flies, gain modulation of visual responses in locusts during flight occurs at the level of descending neurons (Reichert et al., 1985), and it can be expected that

state dependent modulation of compass cells is similarly complex as modulation in the fly optomotor system.

Similar to our data on walking behavior Homberg (1994) showed that bouts of flight activity go along with spike rate changes in locust compass cells. Evidence was presented both for a central signal and proprioreceptive feedback signaling flight activity, as described for cockroach CX neurons during walking (Bender et al., 2010; Martin et al., 2015). Our experiments, likewise, suggest that changes in spike rate occur upon mechanical stimulation of single legs (Fig. 6A,B) and during spontaneous leg movements. To what extent these spike rate changes are caused by proprioceptive input from walking legs and central gain modulation during locomotor activity remains to be established. A multitude of mechanisms reporting the animal's current behavioral and internal state may, in fact, be expected from the large variety of neuronal inputs into the CX expressing a broad range of modulatory neurotransmitters (Pfeiffer and Homberg, 2014).

Acknowledgments: This research was supported by grants from Deutsche Forschungsgemeinschaft (HO 950/21-1 and HO 950/24-1 to U.H.). We thank Martina Kern and Jutta Seyfarth for technical assistance.

Conflict of interest: All authors declare that no conflict of interest exists.

References

Bacon, J., Thompson, K. and Stern, M. (1995). Identified octopaminergic neurons provide an arousal mechanism in the locust brain. *J. Neurophysiol.* **74**, 2739-2743.

Beetz, M. J., el Jundi, B., Heinze, S. and Homberg, U. (2015). Topographic organization and possible function of the posterior optic tubercle in the brain of the desert locust *Schistocerca gregaria*. *J. Comp. Neurol.* **523**, 1589-1607.

Bender, J. A., Pollack, A. J. and Ritzmann, R. E. (2010). Neural activity in the central complex of the insect brain is linked to locomotor changes. *Curr. Biol.* **25**, 921-926.

Berens, P. (2009). CircStat: a MATLAB toolbox for circular statistics. *J. Stat. Softw.* **31**, 1-21.

Bockhorst, T. and Homberg, U. (2015a). Amplitude and dynamics of polarization-plane signaling in the central complex of the locust brain. *J. Neurophysiol.* **113**, 3291–3311.

Bockhorst, T. and Homberg, U. (2015b). Compass cells in the brain of an insect are sensitive to novel events in the visual world. *PLoS One* **10**, e0144501.

Bockhorst, T. and Homberg, U. (2017). Interaction of compass sensing and object-motion detection in the locust central complex. *J. Neurophysiol.* **118**, 496-506.

Brainard, D. H. (1997). The psychophysics toolbox. *Spat. Vis.* **10**, 433–436.

Chiappe, M. E., Seelig, J. D., Reiser, M. B. and Jayaraman, V. (2010). Walking modulates speed sensitivity in *Drosophila* motion vision. *Curr. Biol.* **20**, 1470–1475.

Clements, A. N. and May, T. E. (1974). Studies on locust neuromuscular physiology in relation to glutamic acid. *J. Exp. Biol.* **60**, 673–705.

el Jundi, B., Heinze, S., Lenschow, C., Kurylas, A., Rohlfing, T. and Homberg, U. (2010). The locust standard brain: a 3D standard of the central complex as a platform for neural network analysis. *Front. Syst. Neurosci.* **3**, 3-21.

el Jundi, B., Warrant, E. J., Byrne, M. J., Khaldy, L., Baird, E., Smolka, J. and Dacke, M. (2015). Neural coding underlying the cue preference for celestial orientation. *Proc. Natl. Acad. Sci. USA* **112**, 11395–11400.

Fujiwara, T., Cruz, T. L., Bohnslav, J. P. and Chiappe, M. E. (2017). A faithful internal representation of walking movements in the *Drosophila* visual system. *Nat. Neurosci.* **20**, 72–81.

Gewecke, M. and Hou, T. (1993). Visual brain neurons in *Locusta migratoria*. In *Sensory Systems of Arthropods* (ed. K. Wiese, F. G. Gribakin, A. V. Popov and G. Renninger), pp. 119-144. Basel, Switzerland: Birkhäuser.

Haag, J., Wertz, A. and Borst, A. (2010). Central gating of fly optomotor response. *Proc. Natl. Acad. Sci. USA* **107**, 20104-20109.

Hanesch, U., Fischbach, K. F. and Heisenberg, M. (1989). Neuronal architecture of the central complex in *Drosophila melanogaster*. *Cell Tissue Res.* **257**, 343-366.

Hausen, K. (1981). Monocular and binocular computation of motion in the lobula plate of the fly. *Verh. Dtsch. Zool. Ges.* **74**, 49-70.

Heinze, S. (2017). Unraveling the neural basis of insect navigation. *Curr. Opin. Insect Sci.* **24**, 58-67.

Heinze, S. and Homberg, U. (2007). Maplike representation of celestial *E*-vector orientations in the brain of an insect. *Science* **315**, 995–997.

Heinze, S. and Homberg, U. (2008). Neuroarchitecture of the central complex of the desert locust: intrinsic and columnar neurons. *J. Comp. Neurol.* **511**, 454-478.

Heinze, S. and Homberg, U. (2009). Linking the input to the output: new sets of neurons complement the polarization vision network in the locust central complex. *J. Neurosci.* **29**, 4911-4921.

Heinze, S. and Reppert, S. M. (2011). Sun compass integration of skylight cues in migratory monarch butterflies. *Neuron* **69**, 345–358.

Heinze, S., Gotthardt, S. and Homberg U. (2009). Transformation of polarized light information in the central complex of the locust. *J. Neurosci.* **29**, 11783–11793.

Hengstenberg, R. (1982). Common visual response properties of giant vertical cells in the lobula plate of the blowfly *Calliphora*. *J. Comp. Physiol. A* **149**, 179-193.

Homberg, U. (1987). Structure and functions of the central complex in insects. In Arthropod brain: its evolution, development, structure, and functions (Gupta AP, ed), pp 347-367. New York, USA: Wiley.

Homberg, U. (1994). Flight-correlated activity changes in neurons of the lateral accessory lobes in the brain of the locust *Schistocerca gregaria. J. Comp. Physiol.* A **175**, 597- 610.

Homberg, U. and Würden, S. (1997). Movement-sensitive, polarization-sensitive, and light-sensitive neurons of the medulla and accessory medulla of the locust, *Schistocerca gregaria*. *J. Comp. Neurol.* **386**, 329-346.

Homberg, U., Heinze, S., Pfeiffer, K., Kinoshita, M. and el Jundi, B. (2011). Central neural coding of sky polarization in insects. *Philos. Trans. R. Soc. Lond. B Biol. Sci.* **366**, 680–687.

Horváth, G. (2014). *Polarized Light and Polarization Vision in Animal Sciences*. Berlin, Germany: Springer.

Horváth, G. and Varjú, D. (2004). *Polarization Patterns in Nature and Polarized Light in Animal Vision.* Berlin, Germany: Springer.

Jung, S. N., Borst, A. and Haag, J. (2011). Flight activity alters velocity tuning of fly motion-sensitive neurons. *J. Neurosci.* **31**, 9231–9237.

Kathman, N. D., Kesavan, M. and Ritzmann, R. E. (2014). Encoding wide-field motion and direction in the central complex of the cockroach *Blaberus discoidalis*. *J. Exp. Biol.* **217**, 4079-4090.

Kloppenburg, P. and Erber, J. (1995). The modulatory effects of serotonin and octopamine in the visual system of the honey bee (*Apis mellifera L.*). *J. Comp. Physiol. A* **176**, 119-129.

Longden, K. and Krapp, H. G. (2009). State-dependent performance of optic flow processing interneurons. *J. Neurophysiol.* **102**, 3606–3618.

Maimon, G., Straw, A. D. and Dickinson, M. H. (2010). Active flight increases the gain of visual motion processing in *Drosophila*. *Nat. Neurosci.* **13**, 393-399.

Martin, J. P., Guo, P., Mu, L., Harley, C. M. and Ritzmann, R. E. (2015). Central-complex control of movement in the freely walking cockroach. *Curr. Biol.* **25**, 2795-2803.

Müller, M., Homberg, U. and Kühn, A. (1997). Neuroarchitecture of the lower division of the central body in the brain of the locust (*Schistocerca gregaria*). *Cell Tissue Res.* **288**, 159-176.

Pegel, U., Pfeiffer, K. and Homberg, U. (2018). Integration of celestial compass cues in the central complex of the locust brain. *J. Exp. Biol.* **221**, jeb171207, doi: 10.1242/jeb.171207.

Pegel, U., Pfeiffer, K., Zittrell, F., Scholtyssek, C. and Homberg, U. (2019). Two compasses in the central complex of the locust brain. *J. Neurosci.* (in press) DOI: https://doi.org/10.1523/JNEUROSCI.0940-18.2019.

Pelli, D. G. (1997). The VideoToolbox software for visual psychophysics: transforming numbers into movies. *Spat. Vis.* **10**, 437–442.

Pfeiffer, K. and Homberg, U. (2014). Organization and functional roles of the central complex in the insect brain. *Annu. Rev. Entomol.* **59**, 165–184.

Reichert, H., Rowell, C. H. and Griss, C. (1985). Course correction circuitry translates feature detection into behavioural action in locusts. *Nature* **315**, 142-144.

Rien, D., Kern, R. and Kurtz, R. (2012). Octopaminergic modulation of contrast gain adaptation in fly visual motion-sensitive neurons. *Eur. J. Neurosci.* **36**, 3030-3039.

Rind, F. C. (1990). Identification of directionally selective motion-detecting neurones in the locust lobula and their synaptic connections with an identified descending neurone. *J. Exp. Biol.* **149**, 21-43.

Rind, F. C., Santer, R. D. and Wright, G. A. (2008). Arousal facilitates collision avoidance mediated by a looming sensitive visual neuron in a flying locust. *J. Neurophysiol.* **100**, 670-680.

Rosner, R. and Homberg, U. (2013). Widespread sensitivity to looming stimuli and small moving objects in the central complex of an insect brain. *J. Neurosci.* **33**, 8122-8133.

Rosner, R. and Warzecha, A. K. (2011). Relating neuronal to behavioral performance: variability of optomotor responses in the blowfly. *PLoS One* **6**, e26886.

Rosner, R., Egelhaaf, M., Grewe, J. and Warzecha, A. K. (2009). Variability of blowfly head optomotor responses. *J. Exp. Biol.* **212**, 1170-1184.

Rosner, R., Egelhaaf, M. and Warzecha, A. K. (2010). Behavioural state affects motion-sensitive neurones in the fly visual system. *J. Exp. Biol.* **213**, 331-338.

Sakura, M., Lambrinos, D. and Labhart, T. (2008). Polarized sky light navigation in insects: model and electrophysiology of e-vector coding by neurons in the central complex. *J. Neurophysiol.* **99**, 667–682.

Seelig, J. D. and Jayaraman, V. (2013). Feature detection and orientation tuning in the *Drosophila* central complex. *Nature* **503**, 262-266.

Seelig, J. D. and Jayaraman, V. (2015). Neural dynamics for landmark orientation and angular path integration. *Nature* **521**, 186-191.

Srinivasan, M. V., Lehrer, M., Kirchner, W. H. and Zhang, S. W. (1991). Range perception through apparent image speed in freely flying honeybees. *Vis. Neurosci.* **6**, 519-535.

Stern, M. (1999). Octopamine in the locust brain: cellular distribution and functional significance in an arousal mechanism. *Microsc. Res. Tech.* **45**, 135-141.

Stone, T., Webb, B., Adden, A., Weddig, N. B., Honkanen, A., Templin, R., Wcislo, W., Scimeca, L., Warrant, E. and Heinze, S. (2017). An anatomically constrained model for path integration in the bee brain. *Curr. Biol.* **27**, 3069-3085.

Suver, M. P., Mamiya, A. and Dickinson, M. H. (2012). Octopamine neurons mediate flight-induced modulation of visual processing in *Drosophila*. *Curr. Biol*. **22**, 2294–2302.

Turner-Evans, D. B. and Jayaraman, V. (2016). The insect central complex. *Curr Biol* **26**, R445-R460.

Turner-Evans, D., Wegener, S., Rouault, H., Franconville, R., Wolff, T., Seelig, J. D., Druckmann, S. and Jayaraman, V. (2017). Angular velocity integration in a fly heading circuit. *eLife* **6**, e23496.

Varga, A. G. and Ritzmann, R. E. (2016). Cellular basis of head direction and contextual cues in the insect brain. Curr. Biol. **26**, 1816-1828.

Varga, A. G., Kathman, N. D., Martin, J. P., Guo, P. and Ritzman, R. E. (2017). Spatial navigation and the central complex: Sensory acquisition, orientation, and motor control. *Front. Behav. Neurosci.* **11**, 4.

Vitzthum, H., Müller, M. and Homberg, U. (2002). Neurons of the central complex of the locust *Schistocerca gregaria* are sensitive to polarized light. *J. Neurosci.* **22**, 1114–1125.

Weir, P. T. and Dickinson, M. H. (2015). Functional divisions for visual processing in the central brain of flying *Drosophila*. *Proc. Natl. Acad. Sci. USA* **112**, E5523-E5532.

Weir, P. T., Schnell, B. and Dickinson, M. H. (2014). Central complex neurons exhibit behaviorally gated responses to visual motion in *Drosophila*. *J. Neurophysiol.* **111**, 62-71.

Wolff, T., Iyer, N. A. and Rubin, G. M. (2014). Neuroarchitecture and neuroanatomy of the *Drosophila* central complex: A GAL4-based dissection of protocerebral bridge neurons and circuits. *J. Comp. Neurol.* **523**, 997-1037.

Zar, J. H. (1999). *Biostatistical Analysis*, 4th edn. Upper Saddle River, NJ: Prentice Hall.

Figures

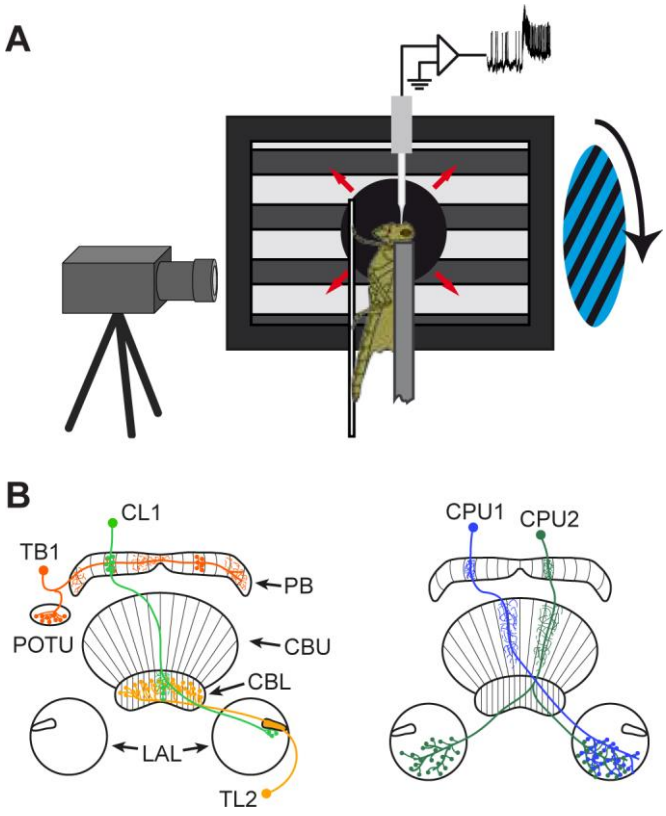

Fig. 1. Recording setup and types of neuron studied. (A) Locusts were tethered in upright posture with hind legs removed and the remaining four legs free to walk on a glass plate with slippery surface. Leg movements were filmed during intracellular recordings from the central brain. The recording electrode was advanced into the central complex from frontal direction. Visual stimulation occurred via two laterally positioned computer screens (only one shown) and via dorsally presented polarized light. (B) Five types of neuron were recorded. Input neurons to the central complex (TL2 cells) and intermediate neurons (CL1 cells, TB1 cells) are shown on the left side and output neurons (CPU1- and CPU2 cells) are shown on the right side. CBL, lower division of the central body; CBU, upper division of the central body; LAL, lateral accessory lobe; PB, protocerebral bridge; POTU, posterior optic tubercle.

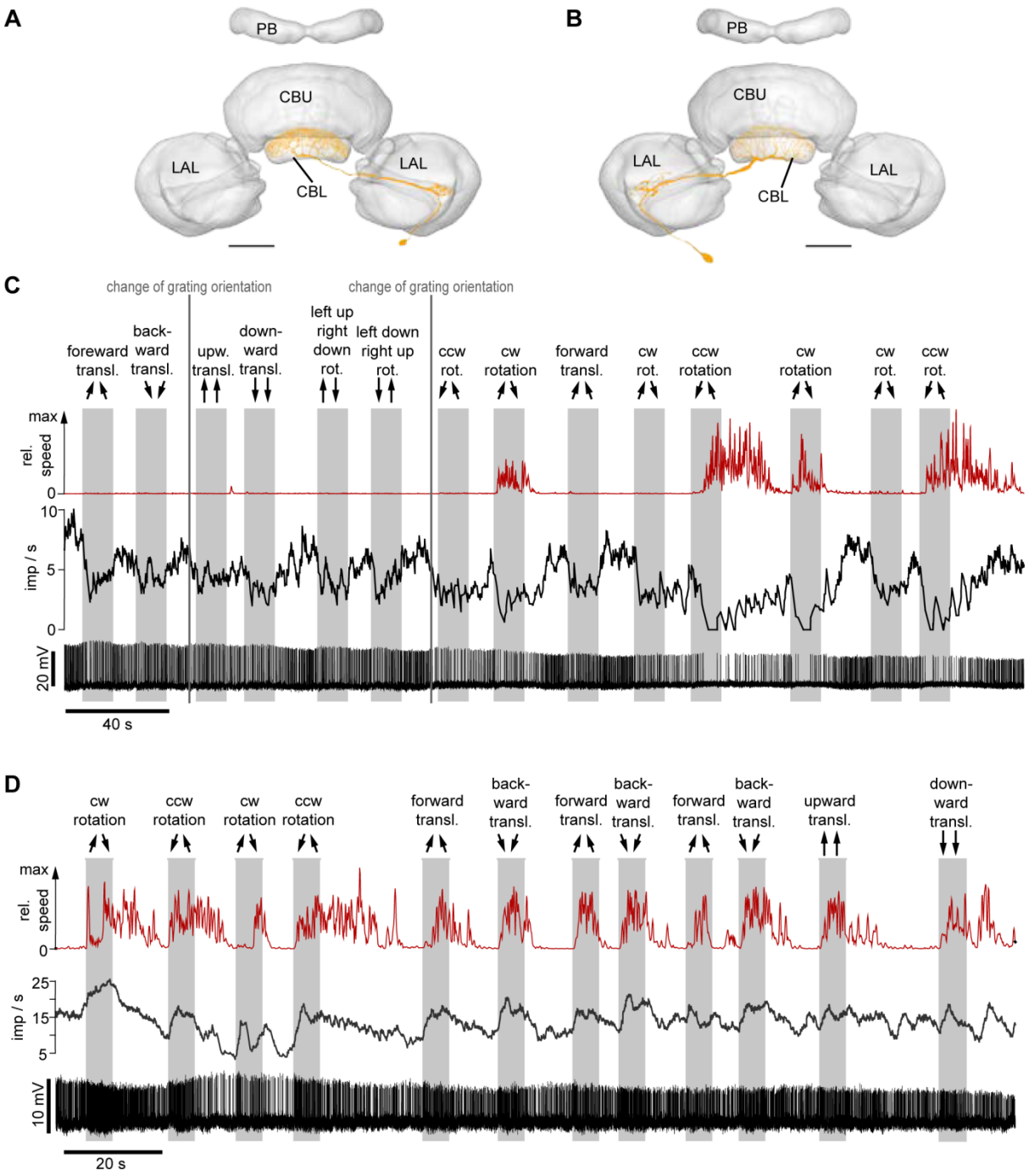

Fig. 2. Activity changes in two TL2 neurons during rotating and translating moving grating stimuli (grey shaded areas). (A,B) Frontal reconstructions of the two TL2 neurons. Both ramify in layer 2 of the lower division of the central body (CBL). CBU, upper division of the central body; LAL, lateral accessory lobe; PB, protocerebral bridge. Scale bars, 100

µm. (C) Physiology of the neuron in (A); (D) physiology of the neuron in (B). (C,D) Moving directions of gratings are indicated on top as seen by the locust. Grey vertical lines in (C) indicate changes of grating orientation during stationary grating phase. In (D) orientation changes coincided with start of grating motion. The 3 traces in (C,D) show (from top to bottom) leg motor activity as summed speed of all 4 freely movable legs, average spiking rate (window size 2 s) and filtered recording trace. cw, clockwise; ccw, counterclockwise; imp, impulses.

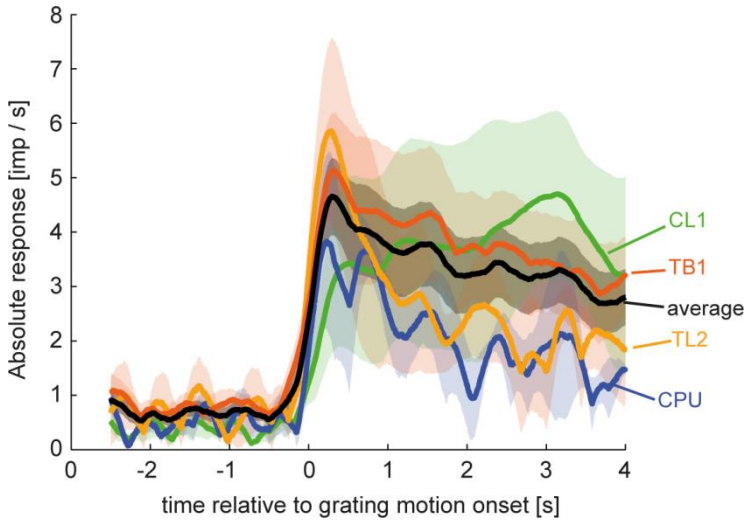

Fig. 3. Responses of compass cells to bilateral, progressive wide-field motion. Traces are averaged Gauss filtered spike trains (± SEM) of responses normalized to activity during stationary grating presentation. Inhibitory responses were inverted before averaging. Stationary gratings presented to the animals started to move at time point 0 ms. Black line shows average absolute response to grating motion for 23 compass cells in the absence of leg motion. Average responses of the different cell types are color coded: three TL2 neurons (yellow), four CL1 neurons (green), 13 TB1 neurons (orange), and three CPU neurons (blue). Ribbons are averages ± SEM.

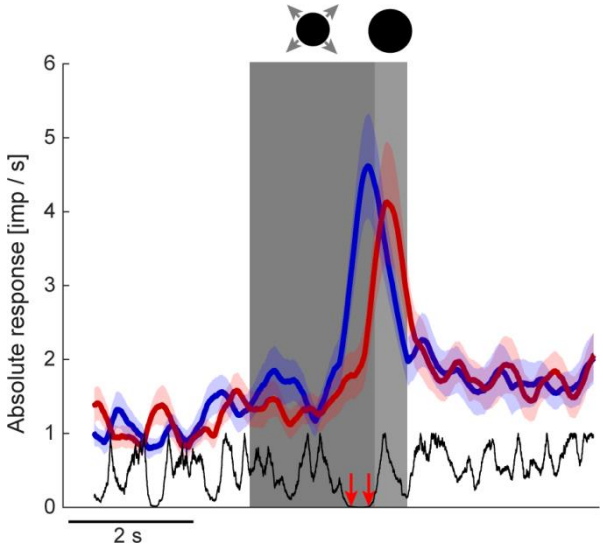

Fig. 4. Average absolute responses of compass cells to looming stimuli in front of a stationary or moving background. Average absolute responses of 18 neurons to monocular looming stimulation are shown in front of a binocularly presented stationary (blue) or moving (red) grating. For 14 neurons both averages contain the responses to looming stimulation of the left and right eye. For the remaining 4 cells the responses from one eye are included only. Ribbons are averages ± SEM. The black line shows p-values calculated with the Wilcoxon signed rank test comparing looming responses in front of moving and stationary gratings. Red arrows indicate start and end of a 265 ms time period with p-values smaller than 0.01. Dark shaded area indicates time span of looming and light grey area, of stationary disc phase, as indicated by the icons above the figure.

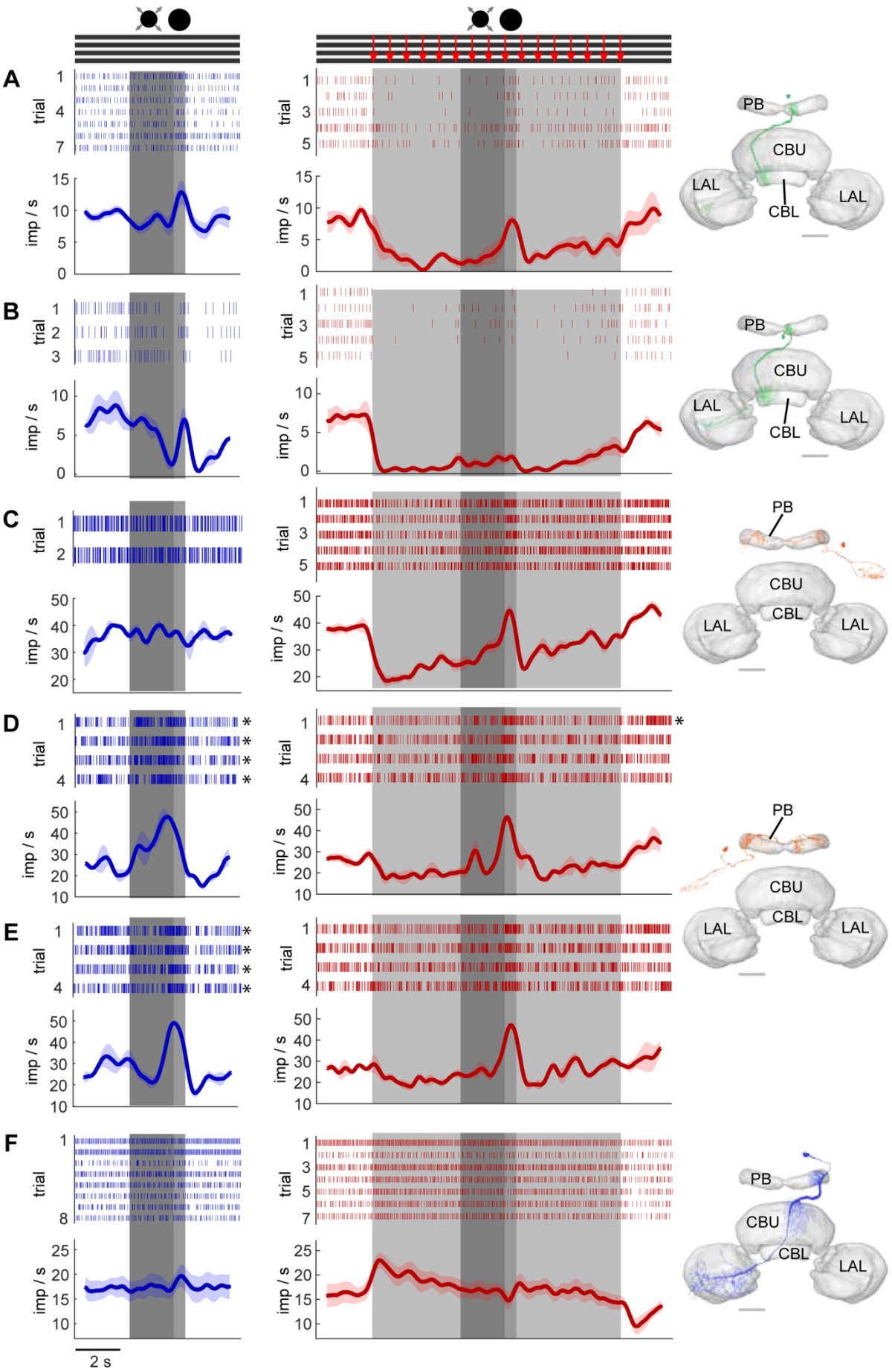

Fig. 5. Responses to looming stimulation in front of a stationary or moving grating. (A-F) Average Gauss filtered traces (± SEM) and raster plots show responses of 5 compass cells to monocular looming stimuli in front of a stationary (left, blue) and a moving grating (middle, red). Right panels show frontal reconstructions of the recorded neurons. Gratings were shown binocularly. Grey shaded areas correspond to looming disc with subsequent stationary disc phase (left and middle panels) and moving grating phase (middle panels), illustrated by icons on top. (A,B) Responses of two CL1 neurons, both innervating slice L1 of the protocerebral bridge (PB) to looming stimulation on the eye contralateral to the neurons' somata. (C-E) Responses of TB1 neurons to contralateral (C,D) and ipsilateral (E) looming stimulation. (C) TB1d neuron (as defined by Beetz et al., 2015) and (D,E) TB1b neuron tested ipsi- (E) and contralaterally (D). (F) Responses of a CPU1 neuron innervating slice R5 of the PB to ipsilateral looming stimulation. Responses in (A-C,F) are without concurrent leg motion, responses in (D,E, left panels**)** and one spike train in (D, middle panel) are with short leg twitches while the disc is looming (traces marked with asterisks). CBL, lower division of the central body; CBU, upper division of the central body; LAL, lateral accessory lobe; PB, protocerebral bridge. Scale bars, 100 µm.

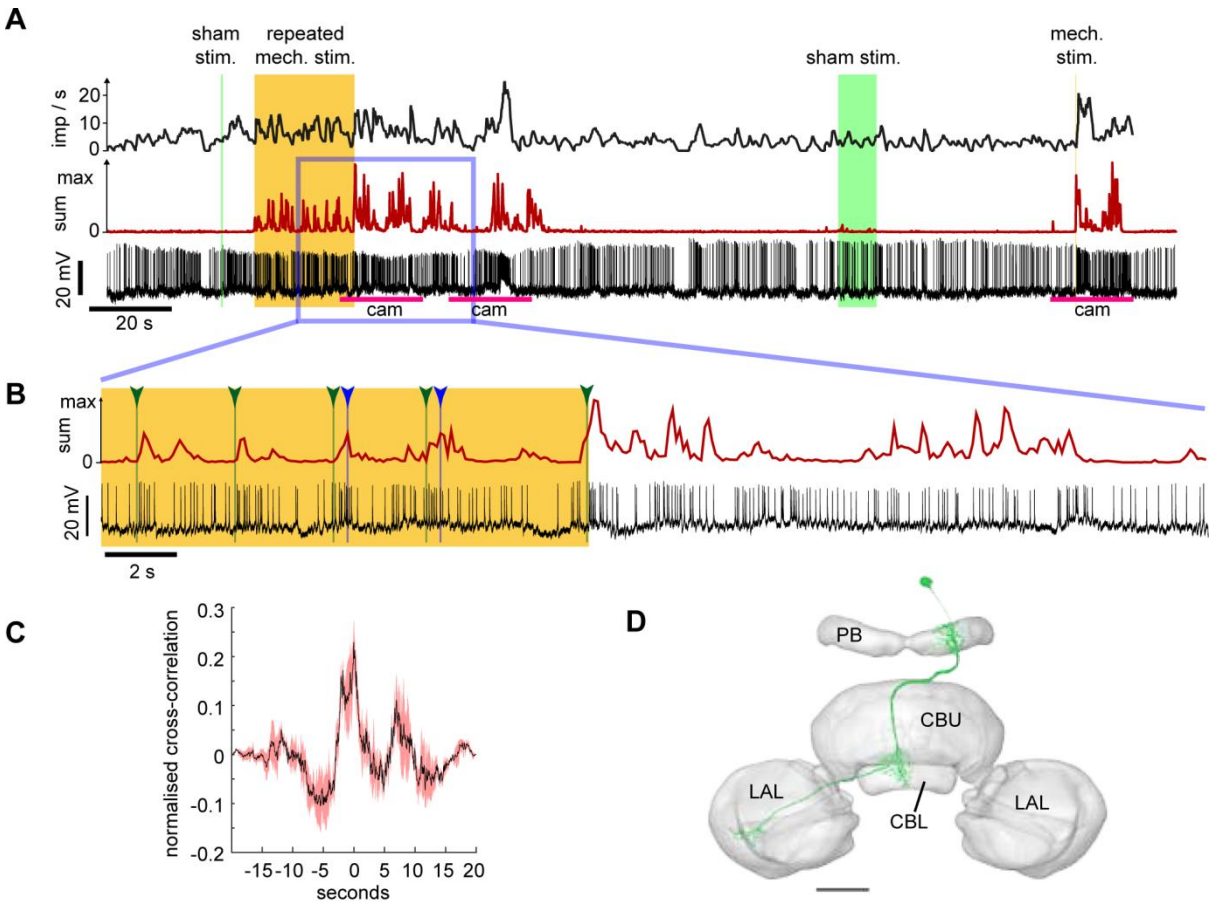

Fig. 6. Effect of spontaneous leg movements and mechanical leg stimulation on the spiking rate of a CL1 neuron. (A) Traces show, from top to bottom, spiking rate, sum of individual leg speeds, and neuronal recording. Small ripples in leg speed traces are due to imperfections in the tracking process of leg movements rather than actual leg movements. Yellow shaded area indicates time of mechanical stimulation, green shaded area, sham mechanical stimulation, i.e. a brush moved in the vicinity of the legs without touching them. Blue frame indicates area enlarged in (B). The pink horizontal lines, labelled with "cam", indicate time periods with high-speed camera recordings for cross-correlogram in (C). (B) Sum of speeds of the four tracked legs and the recording trace. Green lines and arrowheads indicate start of mechanical stimulation of individual legs, blue arrows show stop of stimulation. When only a green arrowhead is present the mechanical stimulation consisted

only of a short tap. All leg movements not highlighted in green occurred spontaneously. (C) Average cross-correlogram (black line) ± SEMs (red shaded area) from three segments of high-speed camera recordings of leg movements (as indicated in (A)) and the corresponding segments of the neuronal recording. (D) Frontal reconstruction of the recorded CL1 neuron. It innervated slice L3 of the protocerebral bridge (PB). CBL, lower division of the central body; CBU, upper division of the central body; LAL, lateral accessory lobe. Scale bar, 100 µm.

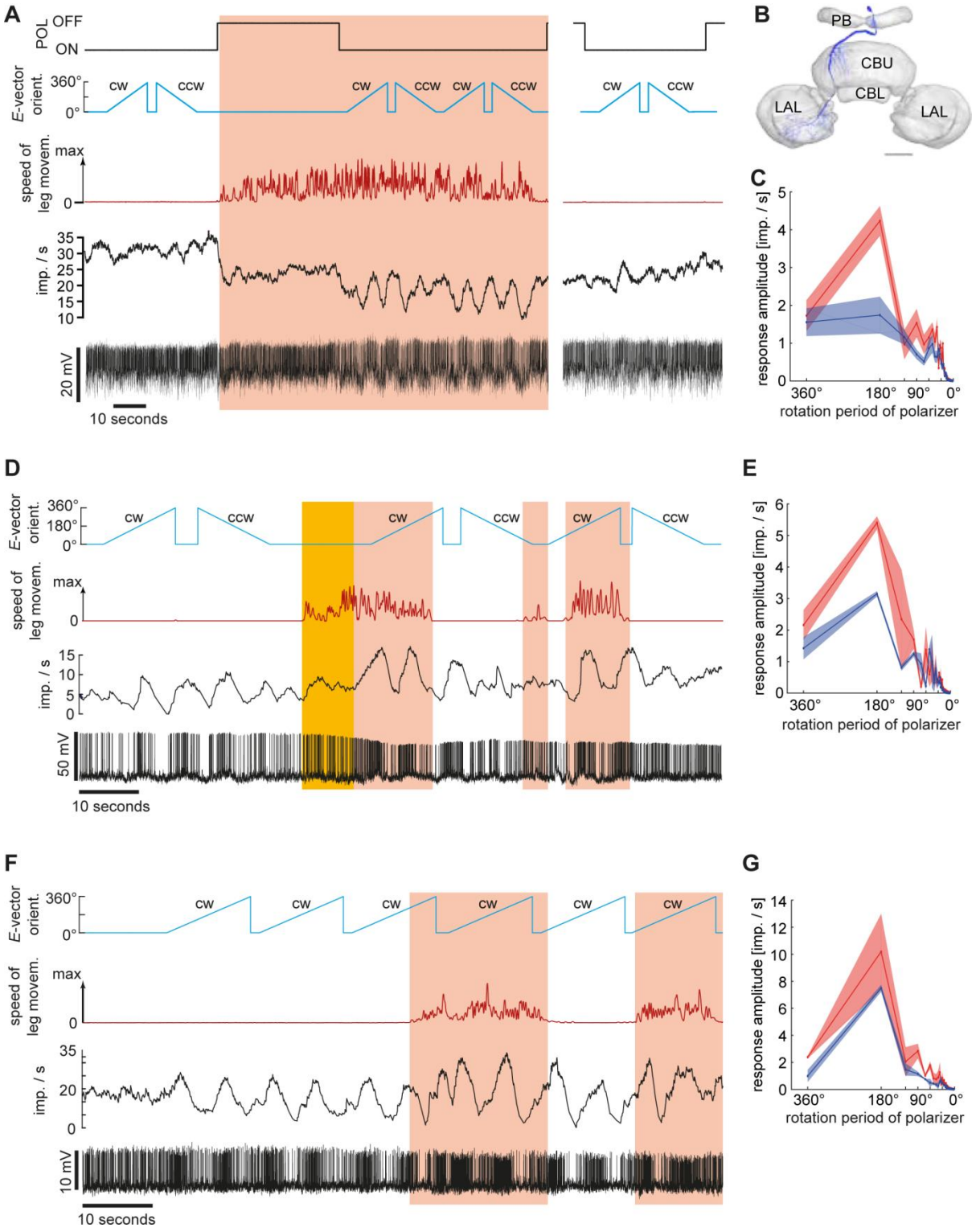

Fig. 7. Effect of motor activity on responsiveness to polarized light. (A,D,F) Periods with leg movements are shaded red. (A) Spiking activity of a CPU1 neuron to polarized light stimulations provided during walking activity and during flanking time intervals without walking. The amplitude of the typical sinusoidal response to the rotating polarizer increases during walking activity. The 8 polarizer rotations were interrupted by tracer injection after the 6th rotation. First trace from top shows times with dorsally presented polarized light switched on or off, second trace, *E*-vector orientation, third trace summed speed of legs, fourth trace spiking rate and fifths trace intracellular recording. (B) Frontal reconstruction of the neuron. It innervated slice L1 of the protocerebral bridge (PB). CBL, lower division of the central body; CBU, upper division of the central body; LAL, lateral accessory lobe. Scale bar, 100 µm. (C) Average (± SEMs) amplitude spectra for walking (n=4, red) and non-walking (n=4, blue) trials. Before calculating the spectra we filtered the spike train with a Gauss filter (SD 200 ms) and subtracted the average spiking rate. (D-G) Recordings from two unidentified CX cells. Summed speeds of leg motion are shown in red. Amplitude spectra in (E,G) as in (C). Number of trials was 2 for each condition. Yellow shaded area in (D) comprises time span of mechanical leg stimulation. cw – clockwise rotation of polarizer, ccw – counterclockwise rotation.

Tables

Table 1. Responses of compass cells to progressive grating motion, looming stimulation and leg motor activity. For visual responses (moving grating and looming responses) only trials without leg motion were analyzed). Trial numbers are provided in brackets. For looming responses, the first number is for left eye and the second for right eye stimulation. If responses for both eyes occurred, they were both inhibitory or excitatory. e, excitation; i, inhibition; -, no response; n/a, not tested or not analyzed because all trials were accompanied by leg movements; n/a in last column means leg movements did not occur. *The looming response during moving grating stimulation occurred for a different eye than the looming response in front of the stationary grating. Responses to leg motion were determined by visual inspection.

Cell ID	Type	Moving grating	Looming on stat. grating	Looming on moving grating	Motor activity
rr121126	TL2	e (6)	e (2/1)	n/a	-
rr121211(Fig. 2A,C)	TL2	i (4)	i (2/3)	- (1/1)	i
rr130911(Fig. 2B,D)	TL2	e (1)	e (3/3)	n/a	e
rr120927	TL2 or CL1	n/a	n/a	n/a	e
rr130926 (Fig. 6)	CL1	e (3)	e (9/24)	n/a	e
rr131004 (Fig. 5A)	CL1	i (7)	e (5/7)	e (3/5)	i
rr140331	CL1	- (10)	e (4/13)	e (3/7)	-
rr141203 (Fig. 5B)	CL1	i (8)	i (1/3)	e (3/5)	n/a
rr131007	TB1	e (4)	e (2/2)	e (1/2)	n/a
rr131021 (Fig. 5C)	TB1	i (8)	- (0/2)	e (0/6)	-
rr140321	TB1	- (6)	- (4/3)	e (3/3)	n/a
rr140322	TB1	- (4)	e (2/1)	- (2/2)	e
rr140324	TB1	- (2)	e (2/1)	e (2/0)	-
rr140326	TB1	i (2)	- (1/4)	- (0/2)	-
rr140328	TB1	i (4)	e (2/3)*	e (1/2)*	n/a
rr140330 (Fig. 5D,E)	TB1	i (8)	n/a	e (3/4)	-
rr140402	TB1	i (2)	- (3/3)	e (3/3)	-
rr141204	TB1	- (11)	e (2/9)	e (3/8)	-

rr141213	TB1	e (15)	n/a	e (1/5)	e
rr141216	TB1	i (10)	i (3/2)	i (4/2)	-
rr141218	TB1	e (14)	i (5/2)	i (5/3)	e
rr131022 (Fig. 7A)	CPU1	- (4)	i (7/2)	- (4/0)	i
rr140323 (Fig. 5F)	CPU1	e (9)	- (8/2)	i (7/2)	-
rr131114	CPU2	- (4)	i (4/1)	i (3/1)	-

Table 2. Amplitude (± SEM) of polarized light responses of 10 neurons during walking and when the animal was motionless. Walking trials were compared with the same number of non-walking trials closest to the walking trials (trial numbers in last column). The amplitude is only given for responses that were statistically significant ($p < 0.05$; see Materials and Methods). NS: non-significant responses.

Cell ID	Cell type	Walking	No walking	Ratio	Trials
rr141204	TB1	2.12 ± 0.36	1.73 ± 0.70	1.23	3
rr140402	TB1	2.98 ± 1.49	2.15 ± 1.38	1.39	2
rr141208	TB1	NS	NS	n/a	2
rr140324	TB1	4.69 ± 0.64	4.77 ± 0.76	0.98	6
rr140323 (Fig. 5F)	CPU1	NS	NS	n/a	4
rr131022 (Fig. 7A-C)	CPU1	4.23 ± 0.39	1.74 ± 0.49	2.43	4
rr131114	CPU2	NS	NS	n/a	1
rr130926 (Fig. 6)	CL1	NS	2.05 ± 0.47	n/a	6
rr131024 (Fig. 7D,E)	not stained	5.40 ± 0.20	3.15 ± 0.08	1.72	2
rr140324_2 (Fig. 7F,G)	not stained	10.19 ± 2.80	7.49 ± 0.25	1.36	2